Silicon Photomultipliers as readout elements for a Compton Effect polarimeter: the COMPASS project

E. Del Monte*[a], A. Rubini[a], A. Brandonisio[a], F. Muleri[a], P. Soffitta[a], E. Costa[a], G. Di Persio[a], S. Di Cosimo[a], E. Massaro[a], A. Morbidini[a], E. Morelli[a], L. Pacciani[a], S. Fabiani[b], D. Michilli[c,d], S. Giarrusso[e], O. Catalano[e], D. Impiombato[e], T. Mineo[e], G. Sottile[e], S. Billotta[f]
[a]INAF IAPS, Via del Fosso del Cavaliere 100, I-00133 Roma, Italy;
[b]INFN sezione di Trieste, Padriciano 99, I-34149 Trieste, Italy;
[c]University of Amsterdam, Science Park 904, 1098 XH, Amsterdam, The Netherlands;
[d]ASTRON, Oude Hoogeveensedijk 4, 7991 PD Dwingeloo, The Netherlands;
[e]INAF IASF-Palermo, Via Ugo La Malfa 153, I-90146 Palermo, Italy;
[f]INAF Osservatorio Astrofisico di Catania, Via S. Sofia 78, I-95123, Catania, Italy

ABSTRACT

COMpton Polarimeter with Avalanche Silicon readout (COMPASS) is a research and development project that aims to measure the polarization of X-ray photons through Compton Scattering. The measurement is obtained by using a set of small rods of fast scintillation materials with both low-Z (as active scatterer) and high-Z (as absorber), all read-out with Silicon Photomultipliers. By this method we can operate scattering and absorbing elements in coincidence, in order to reduce the background.

In the laboratory we are characterising the SiPMs using different types of scintillators and we are optimising the performances in terms of energy resolution, energy threshold and photon tagging efficiency.

We aim to study the design of two types of satellite-borne instruments: a focal plane polarimeter to be coupled with multilayer optics for hard X-rays and a large area and wide field of view polarimeter for transients and Gamma Ray Bursts.

In this paper we describe the status of the COMPASS project, we report about the laboratory measurements and we describe our future perspectives.

Keywords: X-rays, Polarization, Compton effect, Silicon Photomultipliers, Scintillator

1. INTRODUCTION

The measurement of the polarisation of X-rays will add the degree and angle of polarisation to the three observables already gathered in Astrophysics: time, position and energy. Non-thermal emission powering a large majority of X-ray sources, for example synchrotron radiation from electrons, tends to exhibit larger polarization degrees than thermal emission. Another example is the bremsstrahlung process, e.g. from free electrons colliding with ions in a plasma, which emits polarised X-rays[1]. In other cases an unpolarised emission of thermal origin may be polarised via scattering on non-spherically symmetric objects, such as the atmosphere of an accretion disc around a black hole[2].

At low energy X-ray linear polarisation can be measured from the ejection direction of electrons emitted in the detector through photoelectric effect. In fact, a photoelectron is preferentially ejected in the direction of the electric field vector of the incident X-ray. Examples of instruments based on this principle are the gas pixel detector[3,4,5] and the gas micropattern time projection chamber[6]. Instead at higher energy the anisotropy of the distribution of the azimuthal scattering directions in Compton effect becomes dominant. In fact, for linearly polarised photons the Klein-Nishina cross section of the Compton effect depends on the scattering angle θ and the azimuthal angle φ as

*ettore.delmonte@iaps.inaf.it; phone +39 0649934675; fax +39 0620660188; ORCID ID 0000-0002-3013-6334

High Energy, Optical, and Infrared Detectors for Astronomy VII, edited by Andrew D. Holland, James Beletic,
Proc. of SPIE Vol. 9915, 991528 · © 2016 SPIE · CCC code: 0277-786X/16/$18 · doi: 10.1117/12.2232572

$$\frac{d\sigma}{d\Omega} = \frac{r_e^2}{2}\frac{E_1^2}{E_0^2}\left[\frac{E_0}{E_1}+\frac{E_1}{E_0}-2\,(\sin\theta)^2(\cos\varphi)^2\right]$$

where r_e is the classical electron radius (2.8×10^{-13} cm), E_0 is the energy before the interaction and E_1 is the energy after the interaction[7], θ is the angle between the photon direction before and after the interaction (scattering angle), and φ is the azimuthal angle measured from the plane containing both the incoming direction and the electric vector of the incident photon. Thus, from the Klein-Nishina cross section, a linearly polarised photon is preferentially scattered to an azimuthal direction φ orthogonal to the direction of the photon electric field. By accumulating a histogram of the values of the scattering angle θ, in which $N(\theta)$ is the population of each bin, the theoretical modulation factor achievable is defined as

$$\mu(\theta) = \frac{N_{max}(\theta) - N_{min}(\theta)}{N_{max}(\theta) + N_{min}(\theta)}$$

and corresponds to

$$\mu(\theta) = \frac{(\sin\theta)^2}{E_0/E_1 + E_1/E_0 - (\sin\theta)^2}$$

which is highest for scattering at $\theta = 90°$ (see e.g. references[8,9] for more information).

An X-ray polarimeter based on the Compton effect is thus an instrument able to efficiently measure the photon azimuthal direction after the scattering and is most sensitive for a scattering angle of 90°. This instrument shall avoid multiple scattering, which destroys the azimuthal information and thus the polarisation measurement.

It is worth stressing here that the currently available instrumentation exploits the dependence of the cross-section of photoelectric or Compton effects on the photon linear polarisation and is thus able to measure only the linear polarisation.

This paper is organised as follows: in Sect. 2 we describe the framework of this experimental study, in Sect. 3 we describe the experimental set-up, in Sect. 4 we report about the characterisation of the absorption stage, in Sect. 5 we describe the characterisation of the scattering stage, in Sect. 6 we sketch the measurements in coincidence and finally in Sect. 7 we draw our conclusions and give the future perspectives.

2. THE COMPASS PROJECT

COMpton Polarimeter with Avalanche Silicon readout (COMPASS) is a research and development project aiming to measure the polarisation of X-ray photons through Compton scattering. From the previous formulae, in order to measure the polarisation we need to measure the azimuthal angle φ for photons preferentially scattered around 90°. For this reason, we design a polarimeter with a set of scattering elements (or scatterers) made of low-Z scintillators to have a favorable ratio between Compton scattering and photoelectric absorption probabilities, and absorption elements (or absorbers) made of high-Z scintillators to have a high cross section of photoelectric absorption and avoid multiple scattering. Since the scattering and absorption stages are composed of different materials, the proposed design is a two-phases polarimeter following the classification[8]. In COMPASS we aim to use "active" scatterers, to produce a trigger signal from both scattering and absorption elements when interacting with an X-ray photon. For this purpose, all scatterers and absorbers are rods of fast scintillation material, each one individually read-out using a Silicon Photomultiplier (SiPM). SiPMs in scattering and absorption stages are operated in coincidence in order to reduce the background level. We are studying two different configurations for the polarimeter: a focal plane instrument with a single scattering element surrounded by a set of absorbing elements[9] and a large area and large field of view polarimeter for transient sources (e.g. Gamma Ray Bursts) composed of a pattern of scattering and absorption elements[8]. In this phase of the COMPASS project we are focussed on the demonstration of the technology of the two-phases polarimeter with scintillators connected to SiPMs and operating in coincidence.

2.1 Silicon Photomultipliers

SiPMs are photodetectors composed of an array of pixels, each one being a single-photon avalanche diode, operating in Geiger-mode above the breakdown voltage and sensitive to a single photon. All pixels are produced on a common

substrate. The output signal from a SiPM is the analogue sum of the signals from the triggering pixels and is thus proportional to the number of detected photons. SiPMs are currently developed, for example, as read-out sensors for scintillation detectors for applications in medicine, particle Physics and Astrophysics, as well as detectors for Imaging Atmospheric Cherenkov Telescopes.

When compared to photomultiplier tubes (PMTs), SiPMs are more compact and insensitive to magnetic fields, require a bias voltage of the order of only 50 – 100 V and produce faster output signals, with a duration of 0.1– 1 μs. Thanks to a fast development, the SiPMs quantum detection efficiency is rapidly reaching the typical values of PMTs[10]. On the other hand, SiPMs are characterised by a much higher dark current rate than PMTs.

SiPMs are one of the enabling technologies of the COMPASS project. In fact, by using SiPMs as read-out sensors of the scintillation detectors, we can design a compact and light polarimeter as a focal plane instrument and a large area polarimeter for transients with thousands of independent scintillators. In addition, using SiPMs we can operate scattering and absorption elements in coincidence with a time window of only 0.1 – 1 μs in order to reduce the background level. We tested two generations of SiPMs to evaluate their usage for the COMPASS polarimeter. Both of them are produced by the Hamamatsu company, they have a sensitive area of 3 mm × 3 mm and are enclosed in a ceramic package. In this paper we show measurements with the fourth (LCT4) and the fifth (LCT5) generations of Low-Cross Talk SiPMs. We show measurements of LCT4 SiPMs with pitch of 75 μm and LCT5 SiPMs (MPPC S13360-3050CS[1]) with a pitch of 50 μm.

2.2 Plastic scintillator as scattering stage

We recall here that the scattering elements are required to have low-Z to have a favorable ratio between Compton scattering and photoelectric probabilities and a short pulse duration to use a short coincidence time window. For this reason we tested three different types of plastic scintillators produced by the Eljen[2] company and showing these characteristics: EJ-204, EJ-200 and EJ-260. The three materials have a similar light yield of ~10 photons/keV and a pulse duration of few ns. These scintillators are produced as rods with a base of 3 mm × 3 mm (same as the SiPM sensitive area) and heights of 30, 60 and 100 mm, wrapped with teflon tape. The spectrum of the scintillation photons well matches the interval of wavelength with highest photon detection efficiency[10] in the selected SiPMs (380 – 550 nm).

2.3 GAGG as absorption stage

The requirements of the absorption stage are:

- non hygroscopic;
- light emission wavelength compatible with the peak quantum efficiency of SiPMs (380 – 550 nm);
- pulse duration < ~1 μs to "fit" in a narrow coincidence window with the scattering stage;
- high photoelectric quantum efficiency between ~20 keV and ~150 keV;
- high light yield and good spectral resolution;
- vacuum resistant (for space applications).

We chose for the absorption stage a commercially available material which fulfills our requirements, $Gd_3Al_2Ga_3O_{12}$ activated with Ce (hereafter GAGG), produced by Furukawa[3] company. The performances as a gamma-ray spectrometer were studied in reference[11]. The GAGG rods have a square base of 3 mm × 3 mm and a height of 30 mm, and are wrapped with teflon tape.

[1] http://www.hamamatsu.com/jp/en/S13360-3050CS.html
[2] http://www.eljentechnology.com/
[3] http://www.furukawa-denshi.co.jp/english/index.html

3. EXPERIMENTAL SET-UP FOR SINGLE SIPM

3.1 Electronic set-up

We connect the SiPMs to the Hamamatsu C12332[4] driving circuit, composed of two boards: the sensor board, with four sockets to accommodate different types of SiPMs, and the power supply board, providing the bias voltage with temperature feedback. The sensor and power boards are connected with a flat cable of ~5 cm length. Only one SiPM at a time can be connected to the C12332 board.

The C12332 circuit is supplied with ±5 V and can be controlled by a PC via a USB cable. The circuit provides on an SMB output connector the analogue signal from the preamplifier (located in the power supply board). The preamplifier can be excluded and the load resistance can be selected between 50 Ω and 1 kΩ. We used C12332 circuits two different values of the preamplifier gain: 21 (default value) for the absorbing stage and 100 (enhanced value) for the scattering stage.

3.2 Mechanical set-up

We designed and produced a mechanical structure to place the power supply and sensor boards, to hold the scintillator rod in place above the SiPM and to sustain an X-ray source. The sensor board, scintillator and X-ray source are enclosed in a box to reduce the stray light input from the environment. A picture of the experimental set-up is shown in Figure 1.

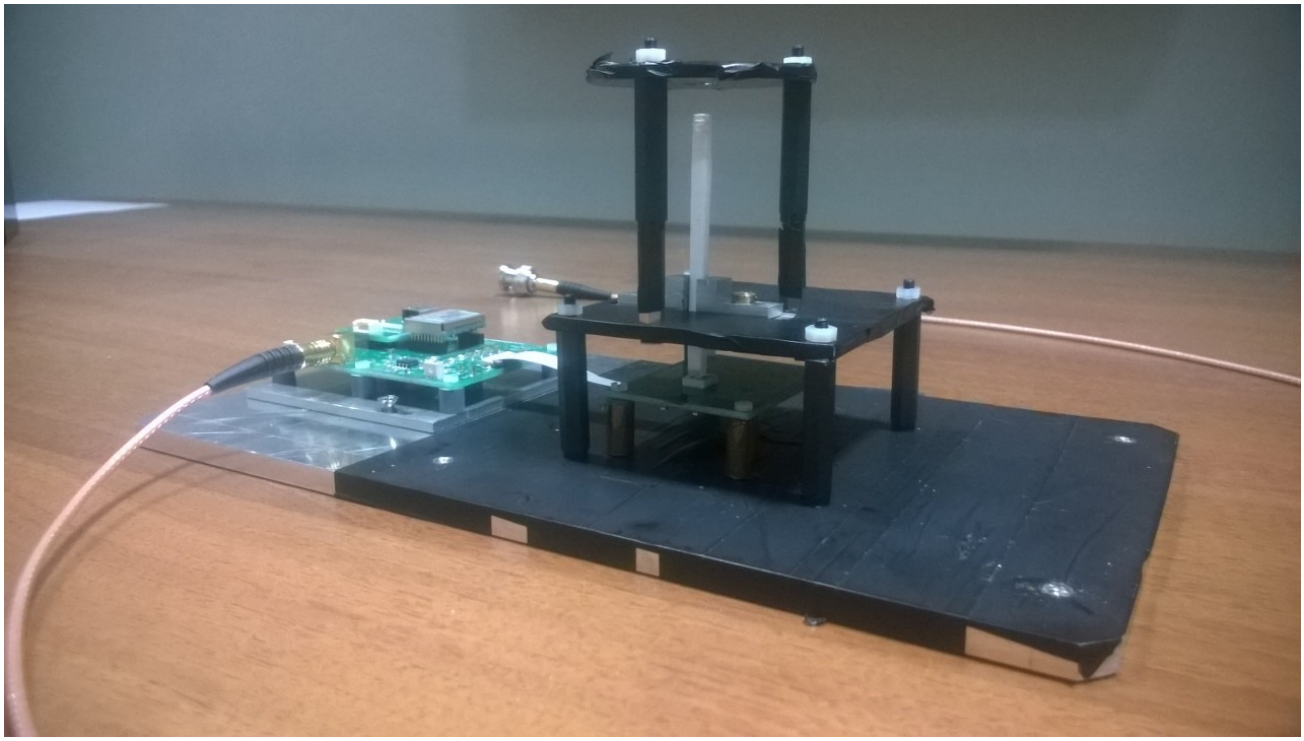

Figure 1: Picture of the experimental set-up. The power supply board is on the left, connected with the flat cable to the sensor board (center). The SiPM is placed on the sensor board, with the plastic scintillator rod (60 mm long) on top. The box to cover the sensor board and the mechanical structure is fixed to the four threaded holes. The black tape is used to reduce the reflection of stray light from the environment.

[4] http://www.hamamatsu.com/jp/en/product/category/3100/4004/4149/C12332-01/index.html

4. CHARACTERISATION OF THE ABSORPTION STAGE

4.1 Objectives and experimental set-up

Since in the Compton effect only a small fraction of the photon energy is deposited in the scattering stage, the absorber detects most of the incident energy. Assuming a Compton scattering angle of 90°, the ratio between the energy of the scattered and incident photon is 96 % at 20 keV, 91 % at 50 keV and 84 % at 100 keV. For this reason we require for the absorber a high quantum efficiency up to high energy, a good linearity over the whole energy range and a good energy resolution.

We measured the linearity and spectral resolution of GAGG from the spectrum of various X-ray lines using an LCT5 SiPM (Hamamatsu 13360-3050CS) with 50 μm pitch and the preamplifier in the C12332 driving circuit with the default gain of 21. We processed the analogue signals from the C12332 circuit using an electronic chain composed of the Research Amplifier Ortec 450 and a multichannel analyser Amptek MCA 8000A. In the measurements we used the mechanical structure in Figure 1.

4.2 Spectra of X-ray sources

We show for example the spectra of X-ray lines accumulated with the GAGG absorption stage: 5.9 keV (from ^{55}Fe, see Figure 2), 22 – 24 keV (from ^{109}Cd, see Figure 3), 59.5 keV (from ^{241}Am, see Figure 4), and 662 keV line from ^{137}Cs (shown in Figure 5). We show in Figure 2 the 5.9 keV line of ^{55}Fe. The dark current rate, partially overlapping with the 5.9 keV line, is empirically modeled with an exponential function. From the system linearity, the valley between the dark current rate and the X-ray line is at 3.3 ± 0.1 keV.

The energy resolution does not allow to resolve the two lines at 22 keV and 24 keV in the spectrum of ^{109}Cd, consequently we fit them with the sum of two Gaussian functions. The parameters of the gaussians are constrained as follows: the position from the energy of the X-ray lines and the area from the branching ratio. We assume the same σ for the two gaussians.

We empirically model the Compton edge on the left of the 662 keV line of the ^{137}Cs source as the product of a Gauss error function and an exponential function (see Figure 5), following the guidelines[12].

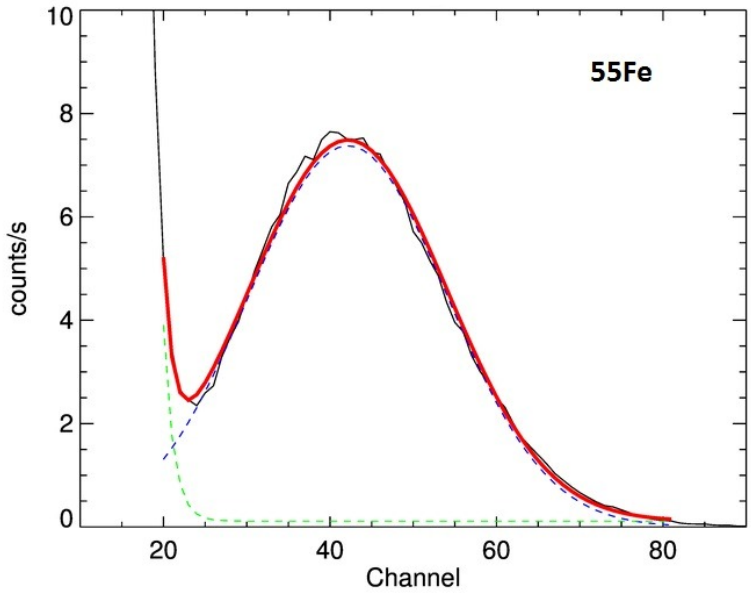

Figure 2: Spectrum of the 5.9 keV line of ^{55}Fe detected with the GAGG rod (3 mm × 3 mm × 30 mm) and the LCT5 SiPM at the nominal overvoltage value of +3 V. The blue dashed line is the gaussian fit of the X-ray line, the green dashed line is the exponential fit of the dark current rate.

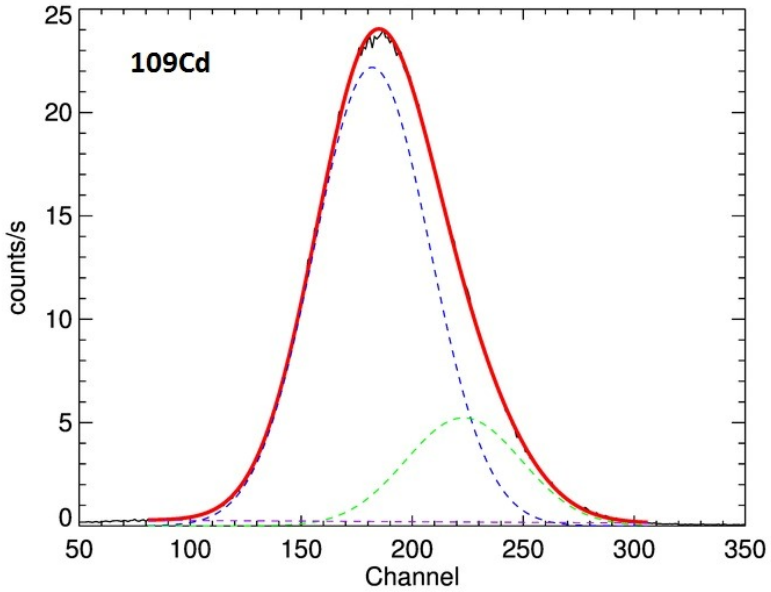

Figure 3: Spectrum of the 22 – 24 keV lines of ^{109}Cd detected with the GAGG rod (3 mm × 3 mm × 30 mm) and the LCT5 SiPM at the nominal overvoltage value of +3 V. The blue dashed line is the gaussian fit of the line at 22 keV, the green dashed line is the gaussian fit of the line at 24 keV, the purple dashed line is the background.

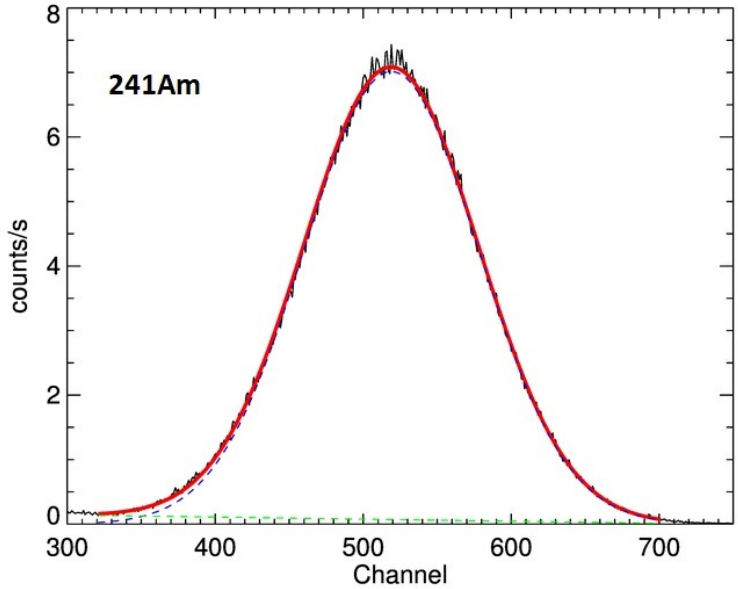

Figure 4: Spectrum of the 59.5 keV line of ^{241}Am detected with the GAGG rod (3 mm × 3 mm × 30 mm) and the LCT5 SiPM at the nominal overvoltage value of +3 V. The blue dashed line is the gaussian fit of the X-ray line, the green dashed line is the background.

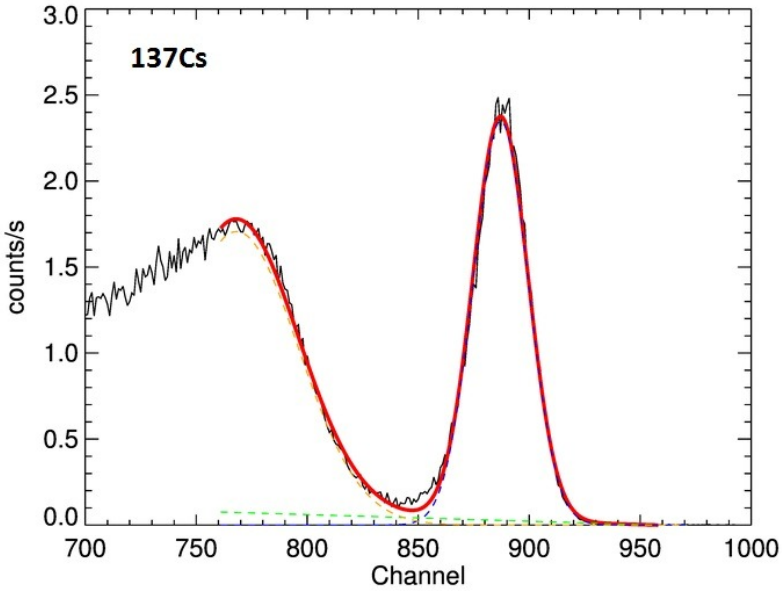

Figure 5: Spectrum of the 662 keV line of ^{137}Cs detected with the GAGG rod (3 mm × 3 mm × 30 mm) and the LCT4 SiPM (75 μm pitch) at the nominal overvoltage value of +3 V. The blue dashed line is the gaussian fit of the X-ray line, the green dashed line is the background and the orange dashed line is the empirical fit of the Compton edge (modelled as the product of a Gauss error function and an exponential function, following the guidelines[12]).

4.3 Linearity of the system and energy resolution

By fitting the spectra in Sect. 4.2 we derived the linearity of the system, i.e. the peak position as a function of energy (shown in Figure 6), and the energy resolution, defined as the ratio between the Full Width at Half Maximum (FWHM) of each line and the peak position (shown in Figure 7).

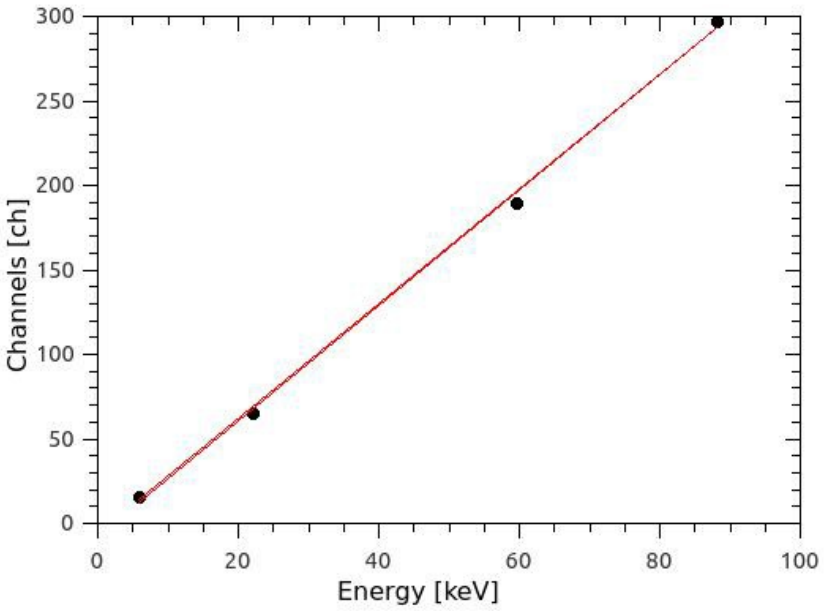

Figure 6: Linearity of the system of GAGG rod (3 mm × 3 mm × 30 mm) and LCT5 SiPM (nominal overvoltage of +3 V).

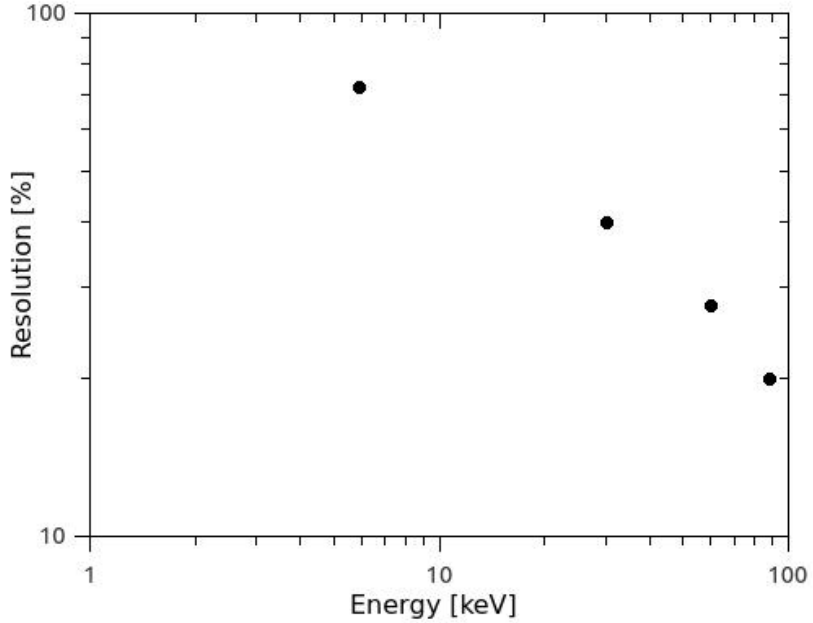

Figure 7: Energy resolution of the system of GAGG rod (3 mm × 3 mm × 30 mm) and LCT5 SiPM as a function of the energy. The energy resolution is defined as the ratio between the FWHM and the peak position.

5. CHARACTERISATION OF THE SCATTERING STAGE

5.1 Objectives and experimental set-up

Our design is based on "active" scattering elements, which are in charge of detecting the electrons scattered in the Compton effect and giving the trigger. For example, a photon of 20 keV Compton scattered at 90° deposits only 0.8 keV in the scattering stage. This is the order of magnitude of the energy on which the scattering stage is required to trigger. For this reason, the lower energy threshold of the scattering stage affects the lower energy threshold of the whole polarimeter.

In this section we report about the measurement of the dark current rate and the light yield for different types of scintillators proposed for the scattering stage, at different values of the SiPM overvoltage. In this characterisation we used the C12332 driving circuit and the internal preamplifier with an enhanced gain of 100. We connected the C12332 circuit to an electronic chain composed of the Timing Filter Ortec 474 and the multichannel analyser Amptek MCA 8000A.

5.2 The dark current

Compared to PMTs, SiPMs show a much higher dark current rate, e.g. of the order of 10^5 cts/s/electron (LCT5 SiPM with 50 μm pitch). As an example we show in Figure 8 the spectrum of the dark current rate measured at room temperature (~22 – 25 °C) without scintillator from an LCT5 SiPM with pitch of 50 μm and overvoltage of +3 V. After calibrating the ADC channels into charge, we derived the dark current rate from the integral of the spectrum from the maximum of the first electron peak up to the maximum of the fourth electron peak (gray area in Figure 9). The value of the integral for different values of the overvoltage is shown in Figure 10.

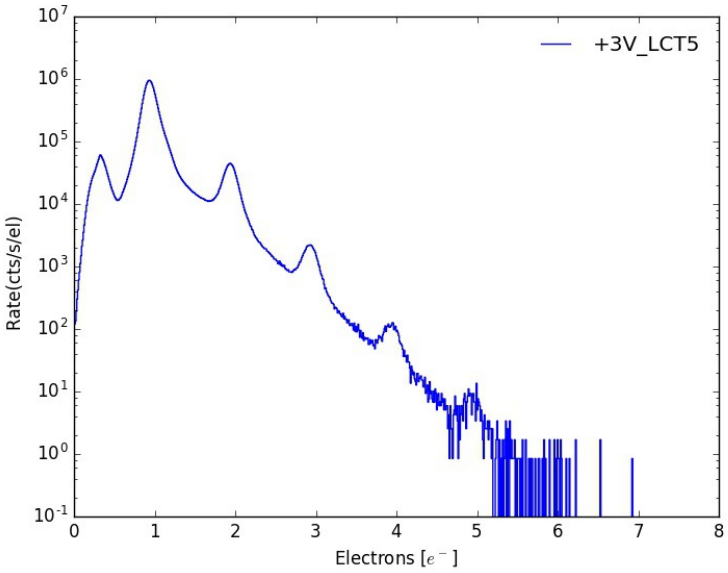

Figure 8: Spectrum of the dark current rate at room temperature (~22 - 25 °C) from an LCT5 SiPM with pitch of 50 μm and overvoltage of +3 V.

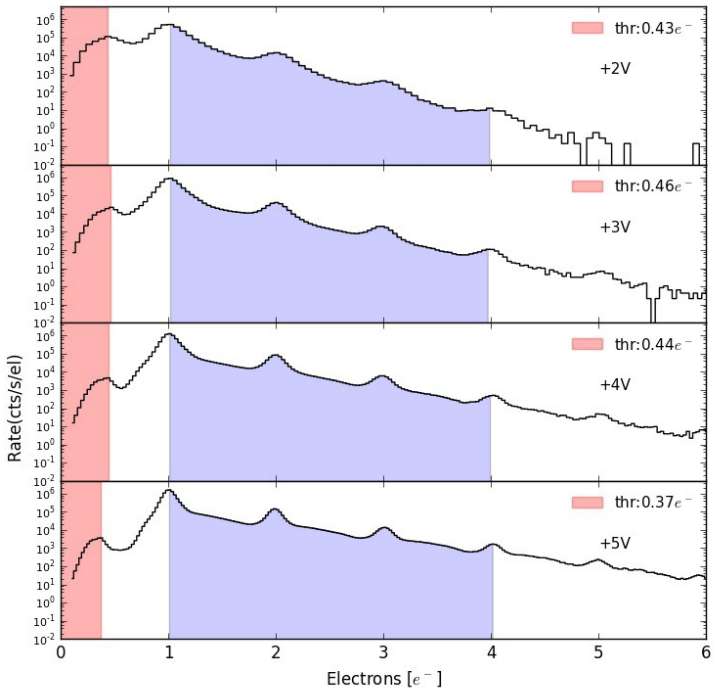

Figure 9: Integral of the spectrum of the dark current rate from an LCT5 SiPM with pitch of 50 μm at different values of the overvoltage (from +2 V to +5 V). The gray area indicates the region of the spectrum considered in the integral.

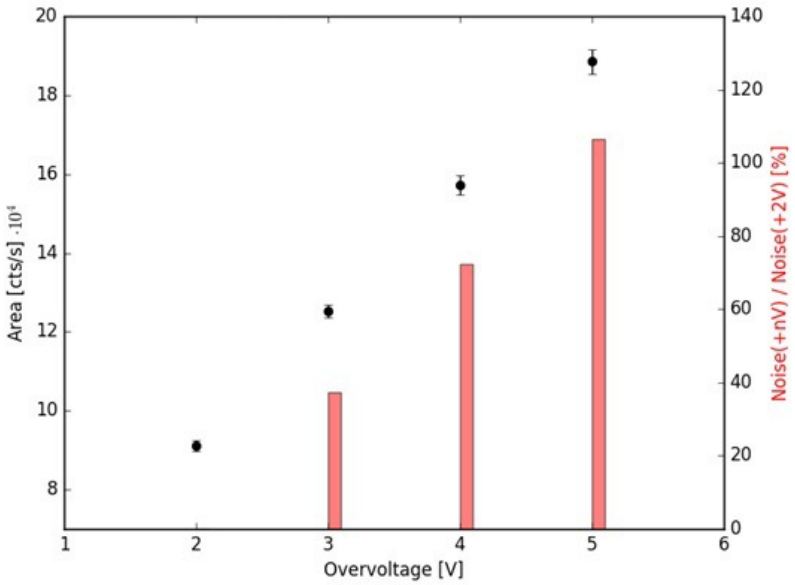

Figure 10: Integral of the dark current rate for different values of the overvoltage in an LCT5 SiPM with 50 μm pitch.

5.3 The light yield

We measured the light yield of the three types of plastic scintillator (EJ-204, EJ-200 and EJ-260) using the 22 – 24 keV line of a ^{109}Cd source. The scintillator rods are connected to an LCT5 SiPM with 50 μm pitch. An example of the spectrum accumulated with EJ-204 at the default overvoltage of +3 V is shown in Figure 11.

The spectrum in Figure 11 is composed of the sum of "narrow peaks", produced by the amplitude of the signal from individual pixels simultaneously triggering. In particular, Figure 11 shows the "narrow peaks" from 5 to 25 pixels simultaneously triggering. We modeled the whole spectrum as the sum of many gaussians, each one corresponding to a "narrow peak" and separately fitted. We find that the FWHM of each gaussian is proportional to $\sqrt{N}$ (where N is the ordinal number of the gaussian), corresponding to the number of pixels simultaneously triggering. Then we fitted with a gaussian the distribution of the area of these "narrow peaks" to find the parameters of the spectrum of the 22 – 24 keV line, summarised in Table 1 for the different plastic scintillators at overvoltage of +3 V.

Table 1: Results of the fit of the spectrum of the 22 – 24 keV line from a ^{109}Cd source for the different plastic scintillators at the overvoltage of +3 V.

Scatterer	Peak position [electrons]	Total rate [cts/s]	FWHM [electrons]
EJ-200	12.8 ± 0.1	240 ± 5	10.4 ± 0.3
EJ-204	13.03 ± 0.04	227 ± 2	10.1 ± 0.1
EJ-260	14.29 ± 0.06	234 ± 3	11.2 ± 0.1

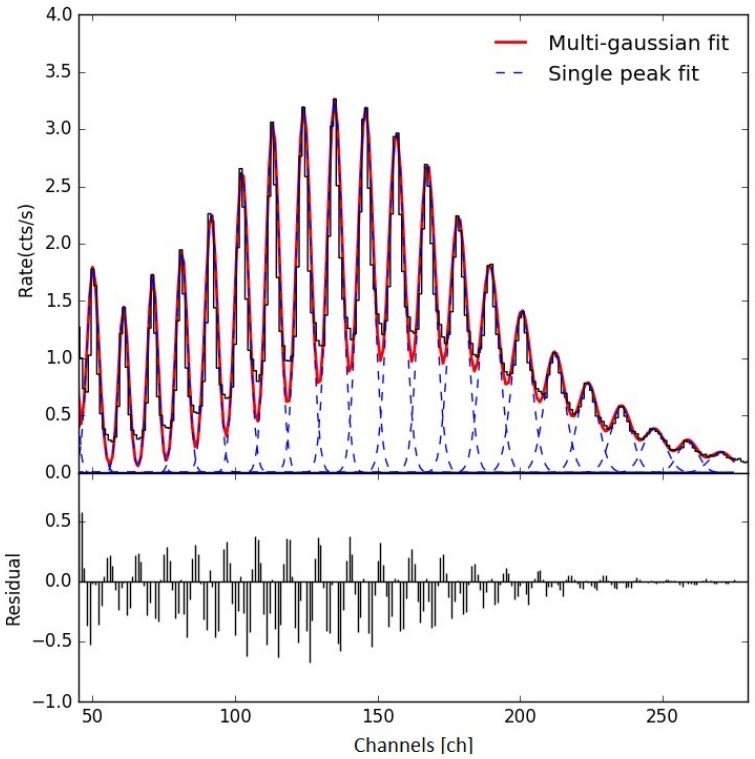

Figure 11: Example of the spectrum of the 22 keV line of ^{109}Cd accumulated with EJ-204 at the default overvoltage of +3 V. Each "narrow peak" is separately fitted. The residuals are due to asymmetries introduced in the peaks by the electronic processing chain.

Assuming to use for the scattering stage the EJ-260, which has the highest measured light yield from the data in Table 1 (0.65 electrons/keV), we expect that an energy deposit of 0.8 would produce an average of 0.5 electrons. From the dark current rate in Figure 8, we expect at 0.5 electrons a dark current rate between ~10^4 and ~10^5 cts/s/electron.

6. TOWARD THE MEASUREMENTS IN COINCIDENCE

The photon tagging efficiency for a system composed of a scattering stage made of the organic scintillator p-terphenyl and an absorbing element made of $LaBr_3$ has been measured in reference[9]. In that case both the scattering and absorbing stages were read-out using PMTs in coincidence. In the framework of COMPASS, we plan to measure the photon tagging efficiency of a single rod of plastic scintillator and a single rod of GAGG read-out using SiPMs operated in coincidence.

In order to study the photon tagging efficiency, we designed and produced a mechanical structure to hold the two C12332 driving circuits with the two SiPMs, the scintillators and the X-ray source. A picture of the mechanical structure is shown in Figure 12. The structure is made of black anodised aluminum to reduce the stray light from the environment.

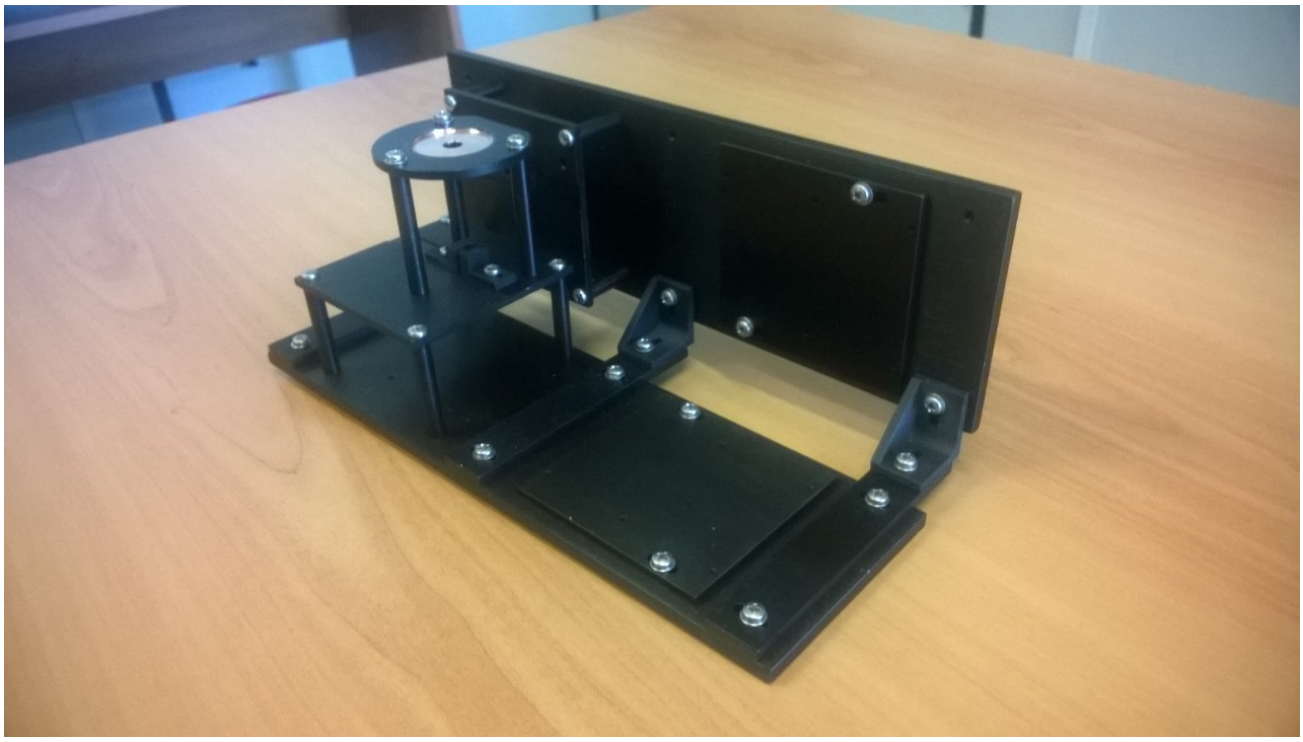

Figure 12: Picture of the mechanical structure for the measurement of the photon tagging efficiency

7. CONCLUSIONS AND FUTURE PERSPECTIVES

We have shown in Sect. 4 the performances of GAGG with a SiPM as read-out element in terms of linearity and energy resolution. We conclude that the GAGG fulfills our requirements and is adequate as absorption stage for COMPASS.

We measured a light yield of 0.65 electrons/keV from the EJ-260 plastic scintillator (see Sect. 5). We have also seen that the SiPM dark current rate allows to detect the signal amplitude below ~1 electron. For this purpose, we need to carefully study the electronic and the coincidence system, since the lower energy threshold of the whole polarimeter is given by the capability to extract signals of amplitude below ~1 electron from the dark current rate.

ACKNOWLEDGEMENTS

The COMpton Polarimeter with Avalanche Silicon readout (COMPASS) project is funded for two years under grant TECNO INAF 2014 by the Italian National Institute for Astrophysics (INAF).

REFERENCES

[1] Motz, J. W. and Placious, R. C., "Bremsstrahlung Linear Polarization" Il Nuovo Cimento 15, 571-572 (1960)
[2] Dovciak, M. et al., "Polarization of thermal emission from accreting black holes" X-ray Polarimetry: A New Window in Astrophysics (Cambridge University Press), 117 (2010)
[3] Costa, E., et al., "An efficient photoelectric X-ray polarimeter for the study of black holes and neutron stars." Nature 441, 662-665 (2001)
[4] Bellazzini, R. et al., "A photoelectric polarimeter for XEUS: a new window in x-ray sky" Procs. SPIE 6266, 62663Z (2006)
[5] Bellazzini, R. et al., "A sealed Gas Pixel Detector for X-ray astronomy" Nucl. Inst. and Meth. in Phys. Res. A 579, 853-858 (2007)
[6] Black, J. K., Deines-Jones, P., Hill, J. E., Iwahashi, T., Jahoda, K., Kaaret, P., Kallman, T. R., Martoff, C. J., Prieskorn, Z., Swank, J., Tamagawa, T., "The GEMS photoelectric x-ray polarimeters" Proc. SPIE 7732, 77320X (2010).
[7] Heitler, W. [Quantum theory of radiation], Oxford University Press, London, (1954)
[8] Costa, E., et al., "Design of a scattering polarimeter for hard X-ray astronomy" Nucl. Inst. and Meth. in Phys. Res. 366, 161-172 (1995)
[9] Fabiani, S., et al., "Characterization of scatterers for an active focal plane Compton polarimeter" Astroparticle Physics 44, 91-101 (2013)
[10] Bonanno, G., et al., "Advances in Multi-Pixel Photon Counter technology: First characterization results" Nucl. Inst. and Meth. in Phys. Res. 806, 383-394 (2016)
[11] Iwanowska, J., et al., "Performance of cerium-doped $Gd_3Al_2Ga_3O_{12}$ (GAGG:Ce) scintillator in gamma-ray spectrometry" Nucl. Inst. and Meth. in Phys. Res. 712, 34-40 (2013)
[12] Cucoanes A. S., "A Toy Model for the Gamma Spectrum Generated in n-Captures on Gd", http://www.yakkas.jp/DChooz/document/AndisFunction/Gd_cucoanes.pdf